Separation & Purification Reviews
Publication details, including instructions for authors and subscription information:
http://www.informaworld.com/smpp/title~content=t713597294

Intraparticle Flow and Plate Height Effects in Liquid Chromatography Stationary Phases

K. H. Hamaker[a]; M. R. Ladisch[a]
[a] Laboratory of Renewable Resources Engineering Department of Agricultural and Biological Engineering, Purdue University, West Lafayette, IN

To cite this Article Hamaker, K. H. and Ladisch, M. R.(1996) 'Intraparticle Flow and Plate Height Effects in Liquid Chromatography Stationary Phases', Separation & Purification Reviews, 25: 1, 47 — 83
To link to this Article: DOI: 10.1080/03602549608006626
URL: http://dx.doi.org/10.1080/03602549608006626

SEPARATION AND PURIFICATION METHODS, 25(1), 47-83 (1996)

INTRAPARTICLE FLOW AND PLATE HEIGHT EFFECTS IN LIQUID CHROMATOGRAPHY STATIONARY PHASES

K. H. Hamaker* and M. R. Ladisch+
Laboratory of Renewable Resources Engineering
Department of Agricultural and Biological Engineering
Purdue University
1295 Potter Center
West Lafayette, IN 47907-1295

Abstract

Velocity independent plate heights were apparently first recognized for hydrodynamic chromatography columns, packed with nonporous, 115 micron glass beads which were run at reduced mobile phase velocities of 10 to 10,000. Hydrodynamic chromatography separates based on the tendency of small molecules (or particles) to associate with slower moving fluid streamlines near the surfaces of particles, compared to larger molecules which seek faster streamlines. Consequently, the larger molecules elute first. Velocity independent plate heights in liquid chromatography have also been observed for nonadsorbed solutes in particulate and fibrous stationary phases. These stationary phases have pores which exceed 10^{-4} to 10^{-5} cm in dimension. The flat plate height is attributed to flow in the channels formed by these large intraparticle spaces. The development of plate height expressions which represent dispersion at interstitial velocities

*Current Address:
Merck & Co., Inc.
P.O. Box 4, WP28B-231
Sumneytown Road
West Point, PA 19486

+to whom correspondence should be addressed.

above 10 cm/min are discussed. Explanations of the uncoupling of dispersion from eluent flow rate in continuous stationary phases, membranes, and gigaporous particles is shown to have their origins in the studies of distribution of particles and molecules in hydrodynamic chromatography columns, and to be adequately described by modifications of the van Deemter equation.

Introduction

Martin and Synge[1] were the first researchers to propose a statistical approach to the experimentally observed phenomena of dispersion of a solute as it migrates through a column packed with silica wetted with water. They adapted the concept of a height equivalent of a theoretical plate as a measure of solute dispersion from previously established conventions for distillation. This was correlated to characteristics of the packed bed, solvent, and solute. Tortuosity, obstruction factors, particle size and shape, solute diffusivity, void fraction, partitioning of the solute between the mobile and stationary phases, and interstitial fluid velocity were later developed as part of the analysis of chromatographic peaks by van Deemter[2] and Giddings[3,4].

Subsequent research has analyzed the effect of rate and equilibrium constants, and the physical characteristics of the stationary phase on the van Deemter model[5]. Solute dispersion is commonly associated with axial dispersion in the interparticulate void volume, and solute diffusional effects in the intraparticle pore volume and convective flow within particles whose pores are on the order of 1 micron. This paper analyzes the basis and utility of plate height and van Deemter type models for relating peak characteristics to combined intraparticle as well as interparticle fluid movement.

Fluid Velocities

A fundamental description of solute dispersivity in packed beds with respect to fluid movement requires clear definitions of fluid velocities. We will

follow the definitions for various fluid velocities[6]. The superficial velocity, u_s, of the mobile phase is obtained from the flow rate, Q, and the cross-sectional area of the empty column:

$$u_s = \frac{Q}{A_o} \tag{1}$$

where

Q = volumetric flow rate (cm^3/min)

A_o = cross-sectional area of empty column (cm^2)

Interstitial fluid velocity, u_e, is the most commonly used measure of fluid velocity for dispersion studies. Interstitial velocity is measured with a molecular probe of sufficient size to be completely excluded from all but the interparticulate voids in the packed bed, and is measured as:

$$u_e = \frac{L}{t_{R,\ excluded}} \tag{2}$$

where

L = axial bed length (cm)

$t_{R,\ excluded}$ = molecular probe (min) retention time of a completely excluded molecular probe (min)

And from comparing superficial and interparticulate fluid velocities, a measure of interparticulate porosity, ε_b, can be found:

$$\varepsilon_b = \frac{u_s}{u_e} \tag{3}$$

Solute movement in the mobile phase is a function of the solute's hydrodynamic shape and volume. The unretained solute velocity, u_{sol}, corresponds to the linear velocity of the solute, or in the case of an adsorbed solute, an unretained molecular probe of similar size and shape, and is defined as:

$$u_{sol} = \frac{L}{t_{R,\ solute}} \tag{4}$$

where

$t_{R,\,solute}$ = retention time of the solute, or unretained probe of similar size and shape (min)

The unretained solute velocity provides a measure of the void fraction accessible to a particular solute. Thus, an unretained solute having a known hydrodynamic radius can be used to determine the void volume of the pores and interparticle spaces which are of sufficient size to permit intrusion by the probe. This can be done for a number of probes of increasing size to provide a measure of the distribution of void volumes ranging from microporous surface structures to macroporous voids between particles. The fraction of bed volume accessible to the solute is defined as:

$$\varepsilon_{sol} = \frac{u_s}{u_{sol}} \tag{5}$$

Chromatographic Plate Height

The dispersion of a solute passing through a uniform packed bed is proportional to the ratio of spread, or variance of the peak, to bed length and is given by the plate height, H:

$$H = \frac{\sigma^2}{L} \tag{6}$$

The plate count, N, is a dimensionless extension of the same ratio,

$$N = \frac{L}{H} = \frac{L^2}{\sigma^2} \tag{7}$$

Conceptually, plate count provides a measure of the column efficiency with a high plate count corresponding to an efficient column. A thorough discussion of plate height and plate count as a measure of dispersion can be found in Hawkes[7].

Plate heights vary with the flow rate of the eluent as illustrated in Figure 1. At low flow rates, the predominant cause of peak dispersion is diffusion. As flow

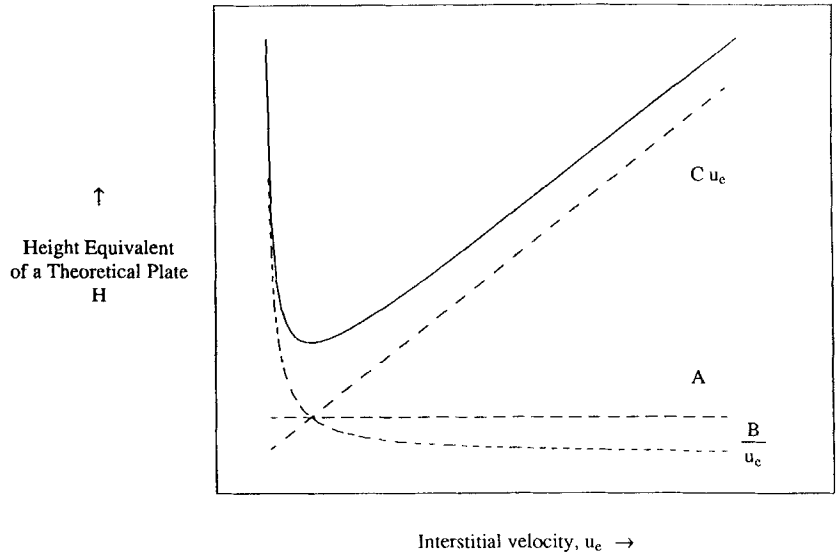

Figure 1. Characteristic Curve of the van Deemter Equation.

rate increases, the axial diffusional contribution decreases, and results in a smaller plate height. But further increases in flow rate cause mixing, and diffusional resistances in the particle pores of the column packing cause plate height to increase again[8,9].

The plate height, or band broadening, in a sorption system is a result of many effects within the bed. These effects may either be diffusional or convective and will be influenced by either physical characteristics of the bed or the flow velocity of the mobile phase in a bed of fixed stationary phase particles.

van Deemter Equation (Velocity Effects on Plate Height)

Plate height for systems with linear equilibrium as a function of interstitial velocity was first described by the van Deemter equation[2]:

$$H = A + \frac{B}{u_e} + Cu_e \tag{8}$$

where

H	=	Height Equivalent for a Theoretical Plate
u_e	=	interstitial velocity
A,B, and C	=	lumped parameters

Equation (8) represents a model which lumps contributions to plate height made by axial dispersion, sorption kinetics of the stationary phase, flow phenomena due to eddy dispersion and flow profile, and mass transfer into the stagnant liquid phase surrounding and within the stationary phase. The first term, A, of the right hand side of Equation (8) represents the contribution of eddy diffusion, also called back flow or wake, occurring as the fluid passes immobile particulates which comprise the packed bed. The term, $\frac{B}{u_e}$, represents longitudinal molecular diffusion in the mobile phase, as well as longitudinal molecular diffusion in the stationary phase for the case of a reversibly adsorbed solute. The term, Cu_e, reflects the dispersion due to sorption-desorption kinetics on the stationary phase and contributions due to diffusion resistance made by solutes diffusing into and out of the pockets of stagnant liquid phase. The terms are additive for linear equilibrium only.

A more fundamental approach to fluid movement is given by the dimensionless quantity, ν, or reduced velocity[6]:

$$\nu = \frac{u_e d_p}{D_m} \tag{9}$$

where

u_e	=	interstitial velocity
d_p	=	characteristic dimension of the stationary phase
D_m	=	Diffusivity of the solute in the mobile phase

The reduced velocity term can be seen as a ratio of molecular diffusion effects and convective effects within the packed bed. D_m can be estimated using the Wilke-

Chang equation[10]. Reduced velocity is important for the development of models to predict plate height as a function of interstitial velocity.

To better compare different plate height models, a dimensionless expression for plate height, h, is given:

$$h = \frac{H}{d_p} \tag{10}$$

Reduced plate heights can be determined as a function of reduced velocity, v. "The theoretical reason (for using reduced plate height and reduced velocities) is simply that identical h, v curves will be obtained from columns which differ only in geometrical scale and nature of eluent used"[11]. All columns do not have the same h vs. υ curves, however. Eluting molecules of different sizes will explore different pore volumes in the particle. Further, the pores may exhibit different diffusional tortuosities, which will further impact the observed plate height.

Other investigators refined the van Deemter equation by incorporating expressions for mechanistic causes of dispersion in LC systems. The lumped form of these models are summarized in Table I[2-4, 8, 9, 11-20] with specific developments discussed in the indicated reference. We have lumped the parameters (A, B, C, D, E) given in Table I in a manner which illustrates the homology between several forms of these equations. The reader is referred to the indicated papers for the descriptions of the lumped parameters as originally defined in these references. The terms which contribute to the plate height expressions are shown in an explicit form in Table II[2,3,4,8,9,14-21].

The Snyder equation[11] is an empirical equation.

$$h = Av^n (0.3 \leq n \leq 0.7) \tag{11}$$

A mechanistic description of the individual plate height contributions was not intended by Snyder and therefore is not included in Table II. However, it should be noted that the Snyder and Knox equations have an advantage over more

TABLE I. Plate Height Models

Citation	Model (solid line in Figure)	Limiting case for large v † (dotted line)	Figure showing Characteristic Curves
van Deemter et al. (1956)[2]	$h = A + \frac{B}{v} + Cv$	$h = A + Cv$	Figure 2
Giddings (1961)[3,4,8,9]	$h = \frac{1}{\frac{1}{A} + \frac{1}{Ev}} + \frac{B}{v} + Cv$	$h = A + Cv$	Figure 3
Snyder (1969)[11,12,13]	$h = Av^n (0.3 \leq n \leq 0.7)$		
Huber and Hulsman (1976)[14,15]	$h = \frac{1}{\frac{1}{A} + \frac{1}{Ev^{1/2}}} + \frac{B}{v} + Cv + Dv^{1/2}$	$h = A + Cv + Dv^{1/2}$	Figure 4
Kennedy and Knox (1972)[16,17,18]	$h = Av^{1/3} + \frac{B}{v} + Cv$	$h = Av^{1/3} + Cv$	Figure 5
Horvath and Lin (1978)[19,20]	$h = \frac{1}{\frac{1}{A} + \frac{1}{Ev^{1/3}}} + \frac{B}{v} + Cv + Dv^{2/3}$	$h = A + Cv + Dv^{2/3}$	Figure 6

† $v = \frac{u_e d_p}{D_m}$, and $h = \frac{H}{d_p}$

TABLE II. Mechanistic Description of Individual Plate Height Contributions

Citation	Interstitial Longitudinal Dispersion: molecular diffusion	Interstitial Longitudinal Dispersion: eddy dispersion	Mass Transfer Resistances: mobile phase	Mass Transfer Resistances: stagnant liquid phase
van Deemter et al., (1956)[2]	$\frac{2\gamma}{v}$	2λ	$\frac{\varepsilon_m^2}{75(1-\varepsilon_m)^2}\frac{1}{(1+k)^2}v$	$\frac{1}{2\pi^2}\frac{k}{(1+k)^2}\frac{\varepsilon_s}{(1-\varepsilon_m)}\frac{D_m}{D_s}v$
Giddings (1961)[3,4,8,9]	$\frac{2\gamma}{v}$	$\Sigma\frac{1}{\frac{1}{2\lambda_i}+\frac{1}{\omega_i v}}$		$\frac{1}{30}\frac{(1-\Phi R)^2}{(1-\Phi)\gamma'}v$
Huber and Hulsman (1967)[14,15]	$\frac{2\varepsilon_m}{\tau_m v}$	$\frac{2\lambda_1}{1+\frac{\lambda_2}{v^{1/2}}}$	$\frac{1}{5.7}\left(\frac{k}{1+k}\right)^2\frac{\varepsilon_m^{1/2}}{1-\varepsilon_m}\left(\frac{v_m}{D_m}\right)^{\frac{1}{6}}v^{1/2}$	$\frac{1}{30}\frac{k}{(1+k)^2}\frac{\varepsilon_m(1-\varepsilon_m)\tau_s}{\varepsilon_s}\frac{D_m}{D_s}v$
Kennedy and Knox (1972)[16,17,18]	$\frac{2\gamma}{v}$	$\frac{1}{\frac{1}{A}+\frac{1}{Cv^n}}\approx Cv^{n(\approx 1/3)}$		$\frac{1}{30}\frac{(1-\Phi R)^2}{(1-\Phi\gamma')}v$
Horvath and Lin (1978)[19,20]	$\frac{2\gamma}{v}$	$\frac{2\lambda}{1+\frac{\omega}{v^{1/3}}}$	$\frac{K(k_o+k'+k_ok')^2}{(1+k_o)^2(1+k')^2}v^{1/3}$	$\left(\frac{1}{30}\frac{\theta(k_o+k'+k_ok')^2}{k_o(1+k_o)^2(1+k')^2}+\frac{2k'D_m}{(1+k_o)(1+k')^2d_p^2k_d}\right)v$
Extended van Deemter (1975)[21]	$\frac{2\gamma}{v}$	2λ	$\omega f(k)v$	$q\frac{k}{(1+k)^2}\frac{D_m}{D_s}\left(\frac{d_f}{d_p}\right)^2v$

Note: See Appendix for notation.

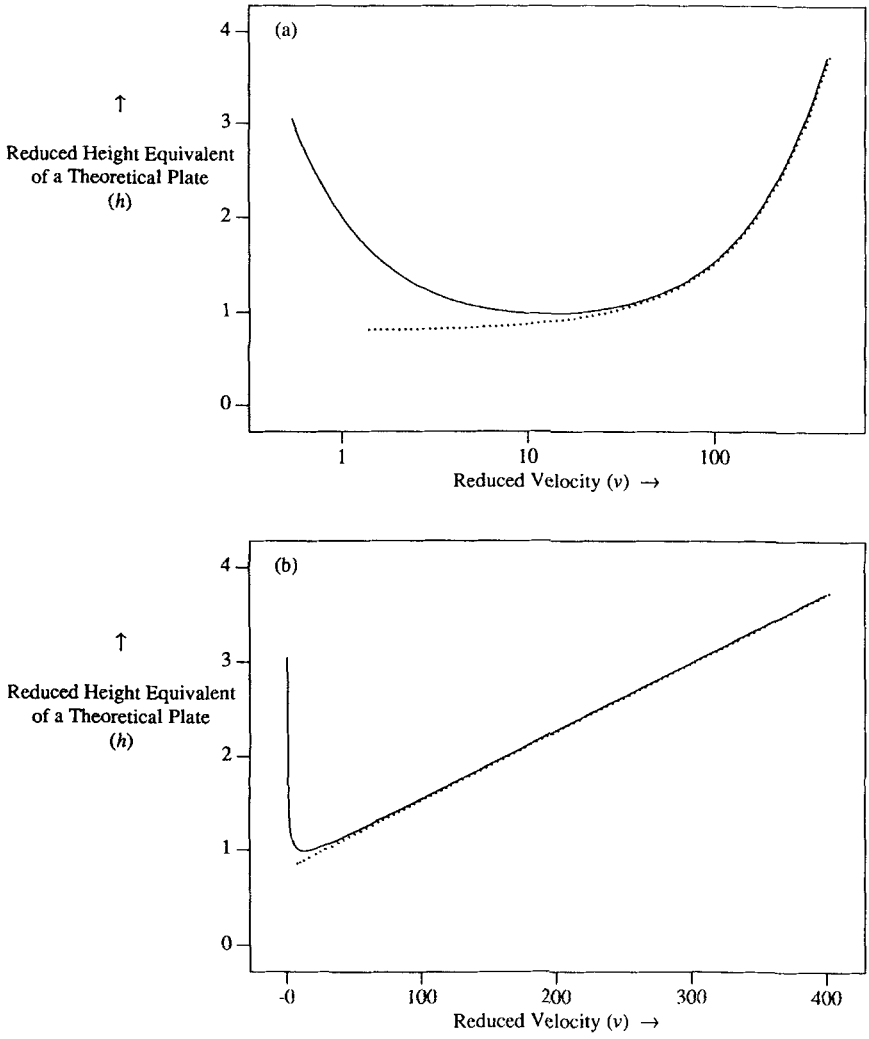

Figure 2. Plot of van Deemter et al.[2] equation showing asymptotic approach of reduced plate height to a constant rate of increase at high velocity. Figure 2(a) shows a log scale representation of reduced velocity, and Figure 2(b) shows v values on a linear scale.

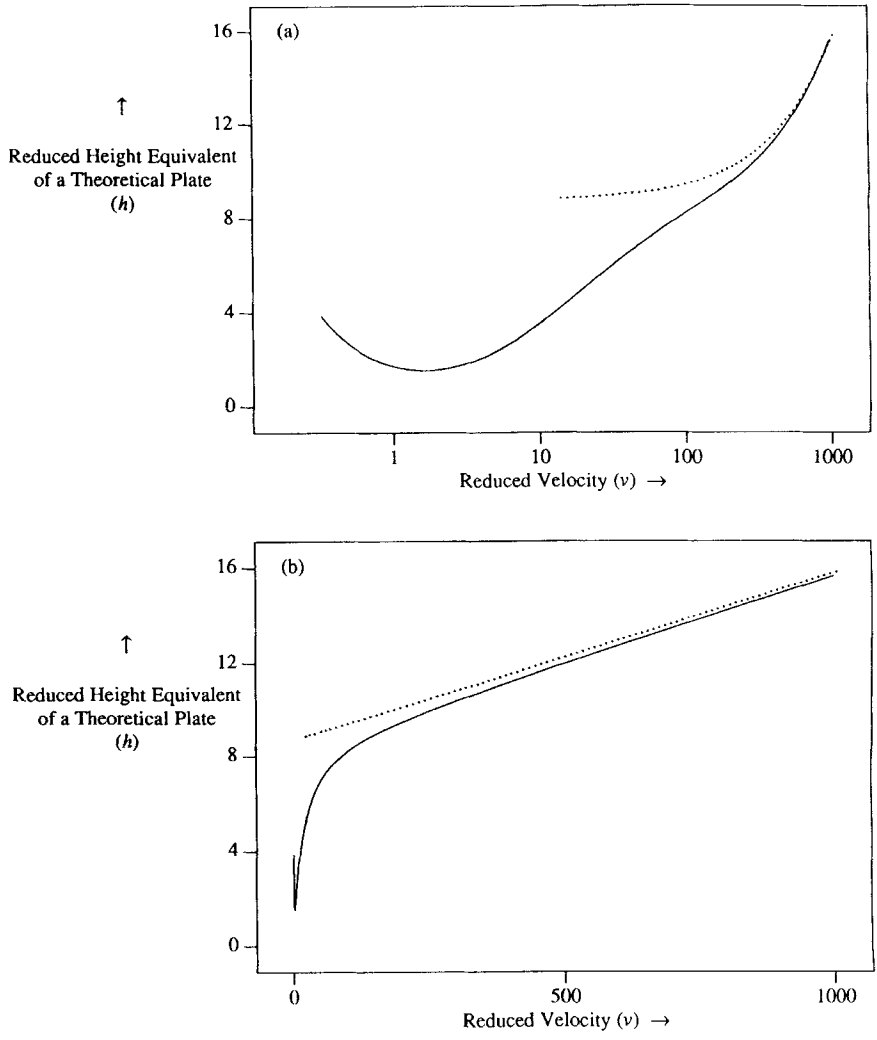

Figure 3. Plot of Giddings[3,4] equation showing approach of reduced plate height to a constant rate of increase at high velocities. Figure 3(a) shows a log scale representation of reduced velocity, and Figure 3(b) shows v values on a linear scale.

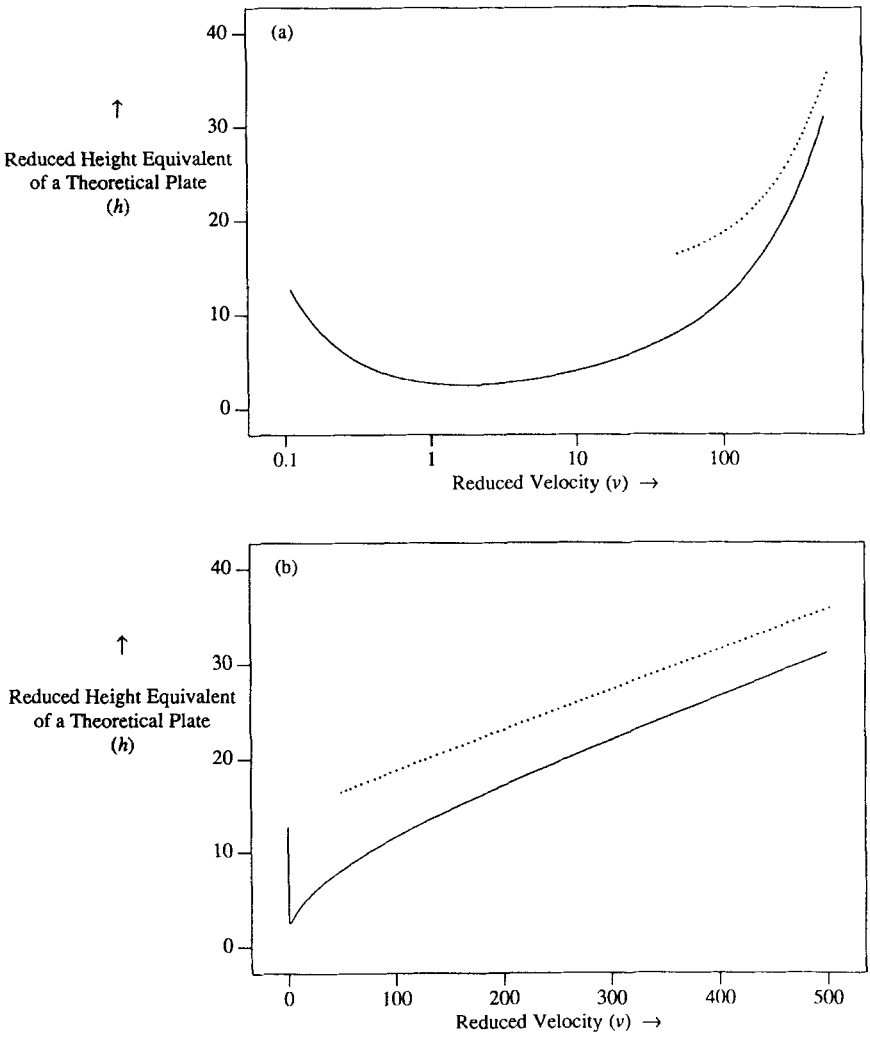

Figure 4. Plot of equation of Huber and Hulsman[14] showing approach of reduced plate height to a constant rate of increase at high velocities. Figure 4(a) shows a log scale representation of reduced velocity, and Figure 4(b) shows v values on a linear scale.

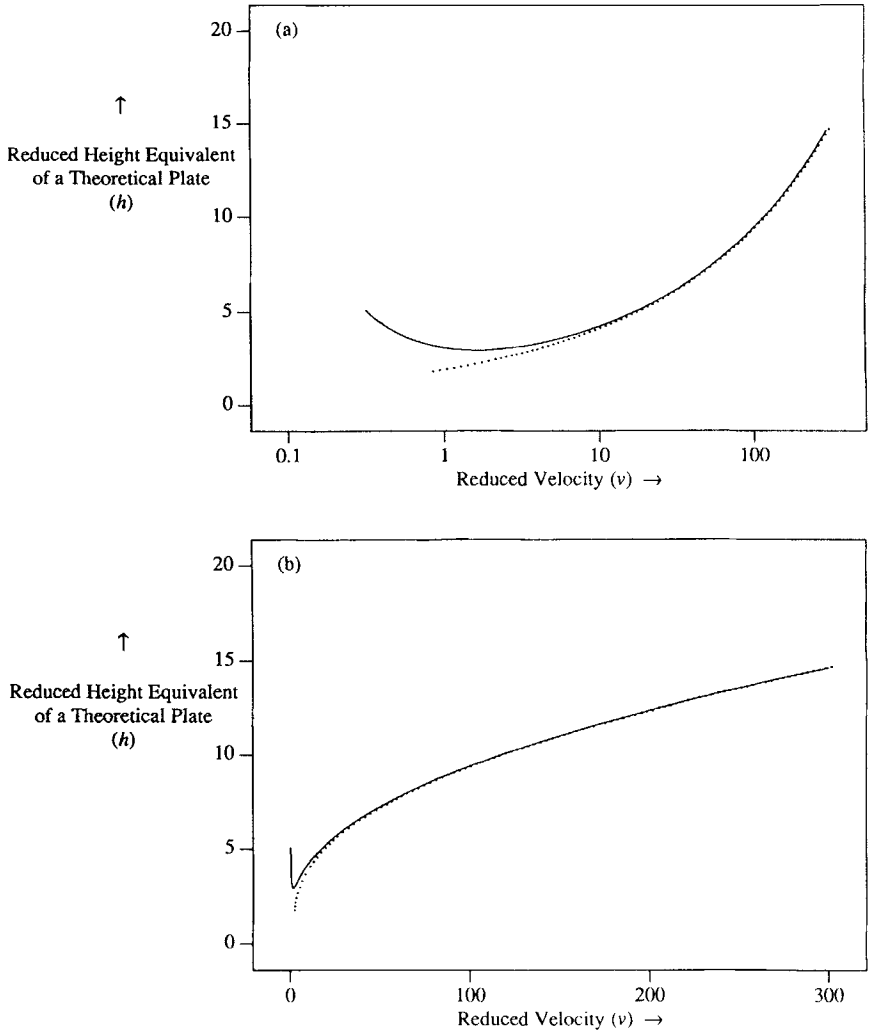

Figure 5. Plot of the Knox equation showing approach of reduced plate height to a constant rate of increase at high velocities (Kennedy and Knox)[16]. Figure 5(a) shows a log scale representation of reduced velocity, and Figure 5(b) shows v values on a linear scale.

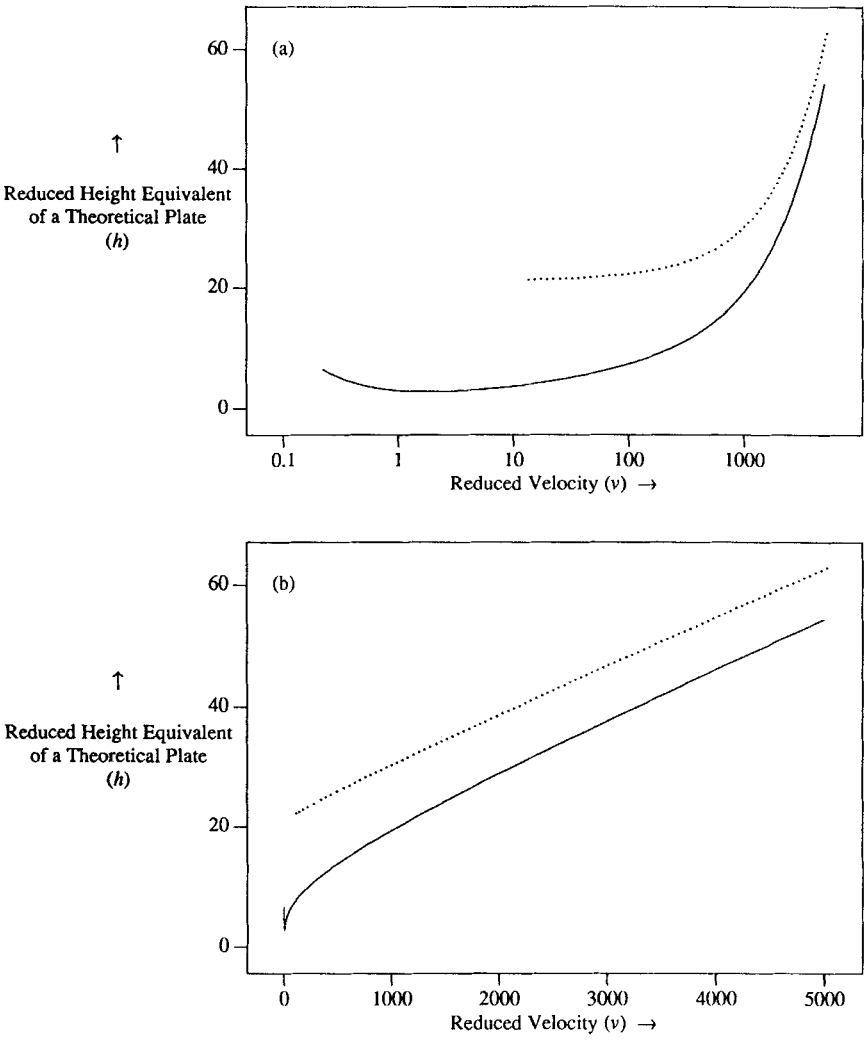

Figure 6. Plot of equation of Horvath and Lin[19] showing approach of reduced plate height to a constant rate of increase at high velocities. Figure 6(a) shows a log scale representation of reduced velocity, and Figure 6(b) shows v values on a linear scale.

involved models because of the ease with which they can be mathematically manipulated for scale-up and design[12,13].

Model Validation

Proper model validation which seeks to discern which model is the true reflection of plate height contributions requires that comparison of H and u_e values be carried out for a sufficiently large range of u_e. Interpretation of the individual terms in each equation may also be necessary. This is laborious since the determination of these parameters requires on the order of one hundred experimental observations for obtaining statistically significant results for each model[22].

For example, a series of 750 experiments were carried out by Katz, et al.[5] for LC columns packed with monodisperse silica particles having diameters of 3.2, 4.4, 7.8, and 17.5 microns, respectively. These authors found that the van Deemter equation (12) gave the best fit of peak dispersion as a function of velocity over the range of 12 to 60 cm/min. Their experiments utilized C_5 to C_{10} alkanes with ethyl acetate as the mobile phase, and benzyl acetate and hexamethylbenzene as the molecular probe.

$$h = 2\lambda + \frac{2\gamma}{v} + \frac{\left(a + bk + ck^2\right)}{24(1+k)^2}v \qquad (12)$$

The values of λ and γ are typically 0.5 and 0.8 but vary with the quality of packing. Values of a, b, and c are 0.37, 4.69, and 4.04, respectively[5,23]. A number of mechanisms cause dispersion and it is difficult to uncouple and test the relative importance of an individual contribution. Because each contribution is defined by a physical process, each lumped parameter must necessarily be real and positive, and have a value which is physically reasonable.

Systems Involving Intraparticle Forced-Convection Hydrodynamic Chromatography

Hydrodynamic chromatography (HDC) describes a separation which is based on convective flow phenomena alone[24]. The stationary phase consists of either capillaries or packed beds of non-porous particles. Like size-exclusion systems, HDC systems separate molecules and colloidal particles on basis of size. However, unlike size-exclusion, where it is assumed that larger molecules are unable to access a certain portion of the bed volume because of steric exclusion, molecules in an HDC system separate because they are excluded from slower streamlines near the particulate surface or capillary wall. Larger molecules are confined to a smaller region at the center of the flow stream than are smaller particles. Consequently, larger molecules elute prior to smaller molecules. It is still a matter of debate whether the confinement of molecules to certain portions of the stream relative to the molecular size is a result of steric exclusion from streamlines near the particle surfaces or capillary walls, or whether the molecules elute in annular rings analogous to "tubular pinching" where the precise annular location of the solute is determined by its size.

Dispersion in hydrodynamic chromatography has been addressed, although a mechanistic description of plate height contributions are apparently unavailable for packed-column hydrodynamic chromatography[25]. Plate height vs. velocity (h, v) curves for these systems have been modeled using the semi-empirical Knox equation:

$$h = Av^{1/3} + \frac{B}{v} + Cv \tag{13}$$

This equation, while useful, is unable to connect causes for solute dispersion with physical parameters of the mobile and stationary phases. However, it is significant to note that Stegeman et al.[25] have also found that when the fluid

velocity exceeds a reduced velocity, ν, of 100 the dispersion becomes independent of the velocity resulting in a constant plate height. This was apparently first observed by Kelley and Billmeyer who used non-porous spherical particles[26].

Gigaporous Particulate Systems

An early example of large pore (i.e., gigaporous) particles is given by the cabbage alumina developed by ALCOA in the mid 1980's. This material, evaluated in our laboratory, consisted of 10 micron alumina, spherical particles with a leaf structure having 1000 to 10,000 Å space between them. These were coated with PEI packed in 0.78 x 10 cm chromatography columns, and run at interstitial velocities of 1 to 15 cm/min. The plate height curves were nearly constant for BSA (MW = 60,000) and IgG (MW > 150,000) over the entire range. The plate height curves were determined using 50 mM Tris-HCl at pH 6.8, containing either 100 mM or 500 mM NaCl. The NaCl was used to supress protein binding, although some adsorption still occurred, even at 500 mM NaCl. This stationary phase, as well as a 1000 Å PEI coated silica was shown to be effective in separating IgG from serum albumin[27,28,29].

Gigaporous particulates (pores > 1000 Å) were reported by Afeyan et al. in 1990[30] as an adsorbent that was capable of intraparticulate convective flow in a chromatography system. These authors coined the term, "perfusion chromatography," to describe this system. Descriptions of solute movement in packed beds for conventional LC systems assumed that pore diffusion was the only form of solute transfer within the particle. Gigaporous systems exhibit increasing intraparticle convection at increasing flow velocities. These are postulated to ultimately become fully convective systems at high flow rates where dispersion becomes constant due to fully formed convective flow within the particulate[31]. The advantage of gigaporous systems, when compared to

conventional LC media, is the increased transfer rates of solutes to the intraparticulate surfaces.

Mathematical modeling of gigaporous particles has addressed both slab and spherical geometries for chromatography media[31]. Researchers have chosen to represent gigaporous particulates as hierarchical systems having an extraparticulate void volume, an intraparticulate void volume (explored under forced convection conditions) and a pore diffusion limited void volume existing within the subparticles. This third void contribution is typically disregarded. Recent experimental measurements by Pfeiffer et al.[43] with single gigaporous particles for gas and liquid flows suggested that the average permeability was independent of particle size, and that the particle behaves as an homogeneous packed bed of microparticles with interstitial channels.

Interpretation of data has relied on establishing a mechanistic relationship between intraparticulate Peclet Number, which is not directly measurable, and the extraparticulate Peclet Number (measured using an appropriately large probe). Frey et al.[32], developed such a model for spherical gigaporous particles comprised of spherical subparticles. Physical characteristics and operational parameters associated with the particles and subparticles are denoted by the superscripts "and", respectively. Similar to the Giddings equation, the total sum of the reduced plate height contributions is given as,

$$h = h_{extra} + h_{ext} + h_{kin} + h_{int} \tag{14}$$

The reduced plate height attributed to extracolumn dispersion, transcolumn flow profile effects, and axial molecular diffusion, h_{extra}, is given as a lumped parameter model,

$$h_{extra} = A + \frac{B}{Pe} \tag{15}$$

and the axial Peclet Number describing interstitial flow is given as,

$$\mathrm{Pe} = \frac{u_e d_p}{D_m} \tag{16}$$

Dispersion due to external mass-transfer, h_{ext}, is given by,

$$h_{ext} = \frac{(1-\alpha)\left(K_{eq}'\right)^2 \alpha^{5/3}}{3.27\left[\alpha + (1-\alpha)K_{eq}'\right]^2} \mathrm{Pe}^{2/3} \tag{17}$$

where α denotes the void fraction associated with the fluid volume which occupies the space between the particulates. The intraparticle distribution parameter, K_{eq}, is given by,

$$K_{eq}' = \varepsilon' + (1-\varepsilon')\left[\varepsilon'' + (1-\varepsilon'')K_{eq}\right] \tag{18}$$

The equilibrium constant, K_{eq}, is,

$$K_{eq} = \frac{\alpha + (1-\alpha)\left[\varepsilon' + (1-\varepsilon')\varepsilon''\right]}{(1-\varepsilon')(1-\varepsilon'')(1-\alpha)} k'$$

where ε', is the void fraction associated with the network of spaces between the subparticles and ε'' is the void fraction associated with the pores of the subparticles, k' is the dimensionless retention factor, $(t_R - t_o)/(t_o)$; t_R is the retention time of the solute; t_o is the retention time of an unretained solute capable of exploring the entire liquid phase; α, ε', and ε'' are the interstitial, intraparticle, and intra-subparticle void volume, respectively. In the case of slow adsorption/desorption systems, the resulting dispersion can be given as,

$$h_{kin} = \frac{3D_m}{8\kappa d_p^2} \mathrm{Pe} \tag{19}$$

where κ is the desorption rate constant. The authors assumed no adsorption occurred ($h_{kin} = 0$). The parameter h_{int} signifies the plate height contribution due to internal mass transfer resistances from hindered diffusion and intraparticulate convection. The internal mass transfer for gigaporous systems involves a convective influence that increases with increasing interstitial velocity. Hence,

the increase in the plate height contribution, h_{int}, is moderated by the velocity dependence of the apparent diffusion constants (equation 21e).

$$h_{int} = \frac{\theta'\alpha(1-\alpha)\left(K_{eq}'\right)^2}{30\varepsilon'\lambda'\left[\alpha+(1-\alpha)K_{eq}'\right]^2}\frac{D_e'}{D_{app}}Pe \tag{20}$$

where

$$u_e' = \left(\frac{d_p''}{d_p'}\right)^2\left(\frac{\varepsilon'(1-\alpha)}{\alpha(1-\varepsilon')}\right)^2 u_e \tag{21a}$$

$$Pe' = \frac{u_e' d_p'}{D_e'} \tag{21b}$$

$$D_e' = \frac{D_m\lambda'}{\theta'} \tag{21c}$$

$$\frac{D_e'}{D_e''} = \frac{\lambda'}{\lambda''}\frac{\theta''}{\theta'} \tag{21d}$$

$$\frac{D_e'}{D_{app}} = \frac{\left[1+\left(\frac{(1-\varepsilon')(\varepsilon'')^2\left(1+K_{eq}\right)^2}{\left[\varepsilon'+(1-\varepsilon'')\varepsilon'\left(1+K_{eq}\right)\right]}\right)\left(\frac{d_p''}{d_p'}\right)^2\left(1+\frac{2Pe'}{45}\right)\left(\frac{D_e'}{D_e''}\frac{\varepsilon'}{\varepsilon''}\right)\right]}{\left(1+\frac{2Pe'}{45}\right)} \tag{21e}$$

where d_p' is the particle diameter and d_p'' is the diameter of the subparticle. Hindrance parameters, λ' and λ'' and tortuosities, θ' and θ'', represent empirical, adjustable parameters.

The model given by equations 14 to 21, indicates the gigaporous system approaches a diffusion controlled system at low Peclet Number. Hindered molecular diffusion would be the chief transport mechanism into and out of the particle. At high Peclet Numbers (> 40) film resistance is a dominant contributor to peak dispersion. A characteristic curve for the Frey expression in equation (14) continues to increase at a high velocity (Figure 7), and dispersion is directly

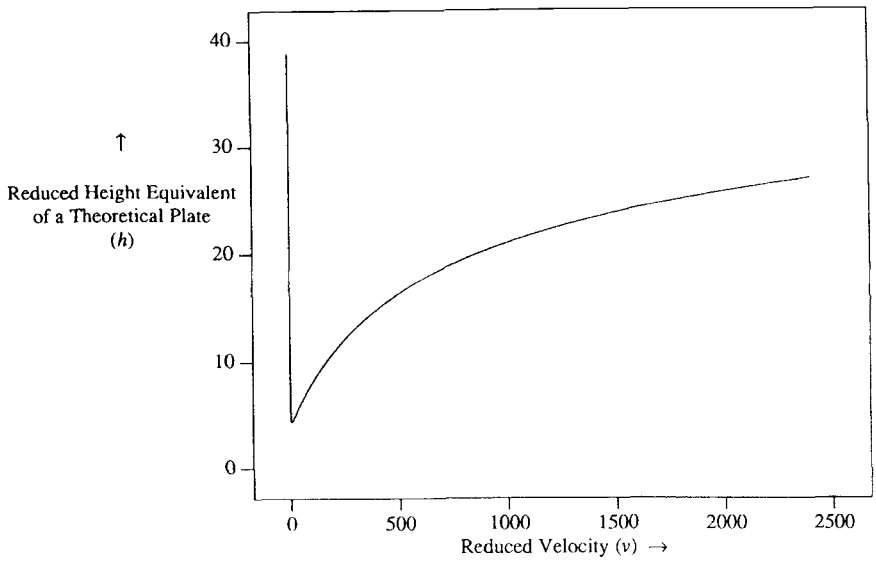

Figure 7. Plot of the Frey et al.[37] expression showing a continued contribution to reduced plate height for increasing flow velocity.

proportional to velocity, although with a smaller slope at reduced velocities above 1000. Previous data[30,32] suggested that the flow velocity should have no influence for gigaporous media at high fluid velocities. This theoretical approach predicts a decrease in the rate at which the plate height increases at high velocity, rather than a constant value.

The movement of the liquid phase and solute in the pore volume has been described as a velocity dependent diffusion process:

$$D_{p,eff} = D_{pore} + u_e D^* \tag{22}$$

where $D_{p,\,eff}$ is the effective diffusion coefficient for a solute molecule within the pore, D_{pore} is pore diffusion coefficient for a stagnant liquid within the pore and D^* is a diffusion coefficient or proportionality constant which reflects fluid

convection within the pore[33]. Axial dispersion due to pore convection and extraparticulate mobile phase flow requires velocity dependent terms to describe the overall dispersion:

$$H = 2A + \frac{2D_m}{u_e} + \frac{1}{30}\frac{k}{(1+k)^2}\frac{d_{pore}{}^2 u_e}{\left(D_{pore} + u_e D^*\right)} \tag{23}$$

The lumped form of this expression has been included in Table III to demonstrate the similarity between this form of coupled effects and that shown by Yang et al.[34] as described for continuous stationary phases. Algebraically, the lumped form of these expressions are the same, predicting a velocity independent plate height value at high velocities. An expression similar to that of equation (22) is given by[30]:

$$D_{p,eff} = D_{pore} + \frac{u_{pore}\, d_p}{2} \tag{24}$$

where u_{pore} is directly proportional to u_e. The expressions in equations (22) to (24) and Table III share a velocity dependent convection term which includes fluid movement within a porous network. This type of model predicts a plate height that will also be velocity-independent at a high enough interstitial mobile phase velocity.

Rodrigues et al.[44] carried out an analysis of large pore supports which presented the apparent effective diffusivity, $\tilde{D}_{eff}$ (which lumps intraparticle diffusion and convection) as[45]:

$$\tilde{D}_{eff} = \frac{D_{eff}}{f(\lambda)} \tag{25}$$

where

D_{eff} = effective diffusivity

$f(\lambda) = \frac{3}{\lambda}\left(\frac{1}{\tanh\lambda} - \frac{1}{\lambda}\right)$

and

TABLE III. Plate Height Models for Intraparticle Convection

Citation	Model	Limiting case for large ν †
van Kreveld and van den Hoed (1978)[33]; Afeyan et al. (1990)[30];	$h = \dfrac{1}{\frac{1}{A} + \frac{1}{E\nu}} + \dfrac{B}{\nu} + F$	$h = A + F$
Yang et al. (1992)[34]	$h = A + \dfrac{B}{\nu} + \dfrac{DC\nu}{D + C\nu}$	$h = A + D$
Carta et al. (1992)[46]	$h = A + \dfrac{B}{\nu} + \overline{C}f(\lambda_R)\nu$	$h = A + \overline{C}$
Rodgiguez et al. (1991, 1993)[44,45]	$H = \dfrac{2L}{Pe} + \dfrac{2}{3}\dfrac{\varepsilon_p(1-\varepsilon)b^2\alpha L}{\left(\varepsilon + b\varepsilon_p(1-\varepsilon)\right)^2}\left[f(\lambda) + \dfrac{3}{Bi_m}\right]$	$H = A + Cf(\lambda)u_o$

† $\nu = \dfrac{u_e d_p}{D_m}$, and $h = \dfrac{H}{d_p}$; u_o = superficial velocity; $f(\lambda) = \dfrac{3}{\lambda}\left(\dfrac{1}{\tanh\lambda} - \dfrac{1}{\lambda}\right)$

λ = intraparticle peclet number ($= v_o \ell / D_{eff}$)

with

ℓ = characteristic dimension (half thickness of slab).

v_o = intraparticle convective velocity.

In this case there is no velocity independent term, although $\tilde{D}_{eff} = D_{eff}$ in the absence of intraparticle convection since $\lambda = 0$ (i.e., $v_o = o$) and therefore $f(\lambda) = 1$.

A similar approach was presented by Carta et al.[46] to describe how intraparticle convection enhances intraparticle transport. These researchers based their mathematical analysis on a uniformly packed bed of permeable spheres with a macroporosity having a sufficiently large diameter so that convective flow occurs inside the particles. Their expression for h is:

$$h = 2\gamma_2 + \frac{2\gamma_1}{\nu} + \frac{1}{30}\frac{(1-\varepsilon)\varepsilon\gamma^2\tau'/\varepsilon'}{[\varepsilon+(1-\varepsilon)\gamma]^2}\nu f(\lambda_R) \qquad (26)$$

Carta et al. state that at large values of ν, the plate height is independent of ν (Table III). In comparison, Rodriguez et al.[44], retain the term $f(\lambda)$ and therefore capture the decrease in plate height, which occurs, for example, in gas-solid systems when intraparticulate convection is present. While a decreasing plate height also results from the analysis of Pretorius and Smuts[47], their equations were developed for gas-liquid and liquid-liquid chromatography in open tubular columns rather than packed beds of particles. The reduction in plate height for their system was predicted to occur at a Reynolds number of 1,000 to 10,000 which corresponds to the transition from a laminar flow profile to a turbulent one in a tube.

Membrane Chromatography

Membrane chromatography systems are comprised of stacked membranes and are typified by small volumes, large surface areas, rapid flow, and short

residence times. The orientation of the membranes and configuration of the flow causes the pores of the filters to become through-pores which promote forced convective flow, thus eliminating any stagnant liquid phase. By removing pore diffusion as an obstacle to solute transport, the only limitation to solute interaction with the surface is film diffusion[35]. As a consequence, mass transfer of the solute to the membrane's surface can be rapid. The absence of pore diffusion enables solutes with identical equilibrium sorption isotherms to be separated via differences between their respective sorption kinetics with the membrane surface[36].

Dispersion in membrane systems has been investigated by Frey et al.[37] using polyvinyl chloride membranes embedded with submicron silica particles and coated with polyethyleneimene. Using a model proposed by Giddings[8], the authors predicted a linear relationship between plate height and flow velocity. However, the data showed the plate height to approach an asymptotic value at high flow rates. Suen and Etzel[38] have shown that the diffusion term in the continuum model can be considered negligible for axial Peclet Numbers above 40. Hence, extracolumn dispersion and dispersion due to the radial flow velocity profile would be dominant causes of peak broadening. These contributions are independent of mobile phase velocity at high flow rates and would lead to a linear increase in plate height for sorbed molecules, and asymptotic behavior for unadsorbed solutes, at high eluent velocities.

Continuous Stationary Phases

Novel stationary phases have been fabricated from rolled woven textile fabric inserted into LC columns. This type of stationary phase has been called a continuous stationary phase (CSP) because each of the individual fibers in the packed bed is by design interconnected with the other fibers in the packed bed. This has led to greater stability and much better flow properties for these fibrous

matrices compared to packed beds of cellulose particulates[34,39]. Subsequent studies have revealed that the resulting dispersion for various solutes used in the operation of CSP becomes linear and independent of flow speed at high velocity.

Yang et al. (1992)[34] noted that plate height was independent of velocity in stationary phases of fibers woven into textile fabrics (i.e., continuous stationary phases) and proposed that a convective effect increased mass transfer in the stagnant mobile phase in the voids associated with intraparticle space. Contributions to plate height made by diffusional and convective effects at the pore can be added in parallel:

$$\frac{1}{H_{pore,\ total}} = \frac{1}{H_{pore,\ convective}} + \frac{1}{H_{pore,\ diffusional}} = \frac{1}{D} + \frac{1}{C'u_{pore}} \qquad (27)$$

where u_{pore}, the velocity through a pore of a discrete particle, would correspond to the interfiber flow in the case of a continuous stationary phase. This mobile phase flow is proportional to interstitial velocity defined in Equation (27), and therefore:

$$C'u_{pore} \equiv Cu_e \qquad (28)$$

Equations (27) and (28) may be rewritten to give the overall plate height of the pore as:

$$H_{pore,\ total} = \frac{DCu_e}{D + Cu_e} \qquad (29)$$

Replacing the previous pore diffusional term, Cu_e, with the right hand side of Eq. (29), a modified van Deemter equation results in:

$$H_{total} = A + \frac{B}{u_e} + \frac{D\,C\,u_e}{D + C\,u_e} \qquad (30)$$

Thus, it is possible to anticipate that the value of H_{total} stays constant as u_e increases above a transitional value determined by the conditions $u_e >> B$ and Cu_e

>>D. When these conditions are met, H_{total} in Eq. (30), approaches a constant value,

$$H_{total} \sim A + D \tag{31}$$

The trend in plate height as a function of reduced velocity is illustrated in Figure 8, although this does not capture the decrease in plate height as a function of large increasing velocities observed by Yang et al. for D_2O[34]. Carta et al.[46] as well as Rodriguez et al.[44] give generalized van Deemters equations which encompass an intraparticle Peclet number $(= v_o \ell / D_{eff})$ and give a flat plate height over a range of capacity factors in a gas-solid and liquid-solid systems (Table III). The analysis of Rodriguez when applied to a gas-solid system shows that a decreasing plate height may occur for large, increasing velocities when superficial velocities exceed 600 cm/min, and when the particle's pores are large enough to permit intraparticle convection[44].

Impact of Uncoupling of Dispersion and Eluent Flow Rate in Continuous Stationary Phases, Membrane Chromatography Systems and Gigaporous Particles

Continuous stationary phases, chromatographic membranes, and nonporous and gigaporous particles minimize the fraction of stagnant fluid in liquid chromatography columns. A common characteristic of such columns is their approach to, or attainment of, a constant plate height at high flow rates for nonsorbing solutes. We estimate that an approach constant plate will begin to occur at approximately v = 100 to 200 (Table IV)[40,41,42]. The uncoupling of solute dispersion from interstitial velocity reflects the dominant effect of film diffusion and sorption kinetics on the rate processes which define solute/sorbent interactions in liquid chromatography columns. The realization that liquid chromatography stationary phases can be designed so that plate height is

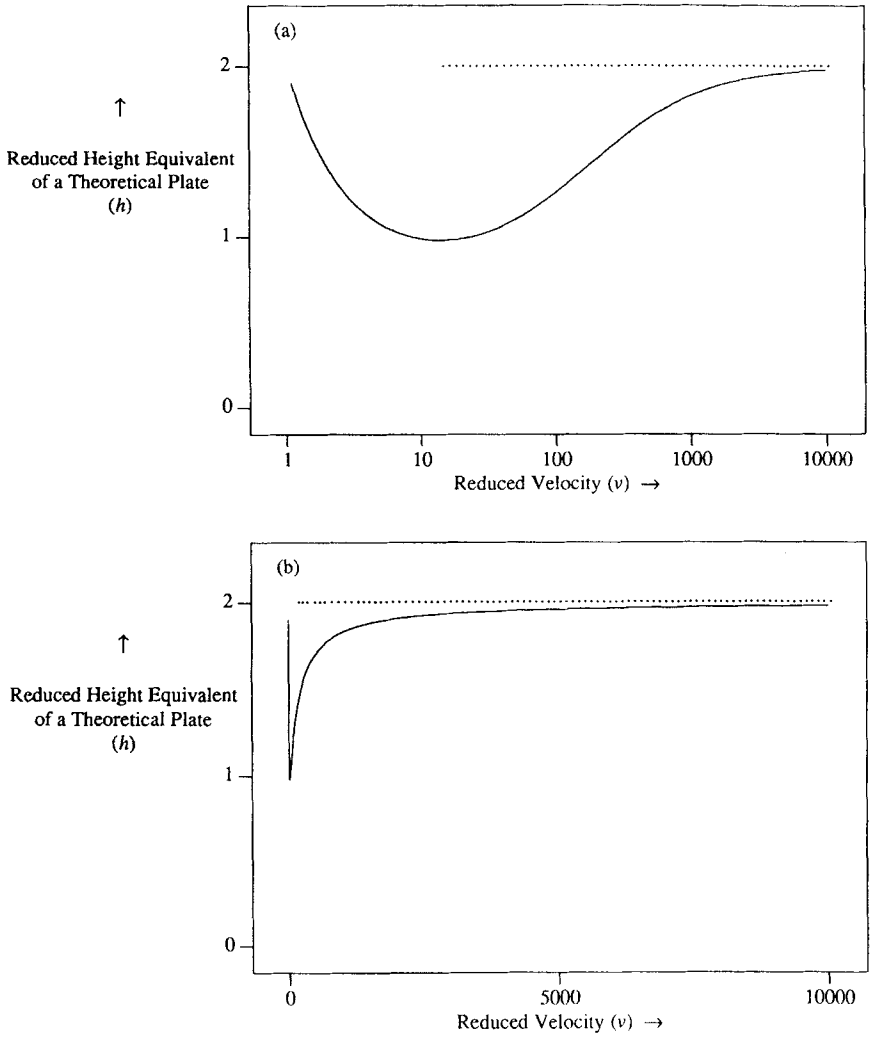

Figure 8. Asymptotic value of plate height approaches a constant when reduced plate height contributions from forced convection are coupled with that of diffusion (van Kreveld and van den Hoed[30], Afeyan et al.[33], and Yang et al.,[34]). Figure 8(a) shows a log scale representation of reduced velocity, and Figure 8(b) shows v values on a linear scale. Solid line is model, dotted line is the limiting case.

TABLE IV. Conditions for Constant Plate Height

Reference Number	Figure in Reference showing data	Solute++	Solvent+++	d_p [cm]	$Dm\left[\frac{cm^2}{s}\right]^{\ddagger}$	ν
34	11	PEG 20,000	H_2O	10×10^{-4} (fiber)		238
26	4	PS 10,300	toluene	115×10^{-4}	$S_c = 3500$	350
	7	PS 3600	toluene	68×10^{-4}	$S_c = 1920$	192
25	5	PS 775000	THF	1.5×10^{-4}	1.65×10^{-7}	70
40	1a	PS 336000	ACN	2.67×10^{-4}	2.64×10^{-7}	152
32	11	lysozyme MW = 14,300	70% ACN 0.1% TFA	8×10^{4} (8×10^{-5} subparticle)		400

\+ Based on interstitial velocity

++ PS = polystyrene
PEG = polyethylene glycol

+++ THF = tetrahydrofuran; ACN = acetonitrile

‡ The diffusivity of polyethylene glycol was determined using published data[41,42]. The linear relationship between the log-values of molecular weight and diffusivity will result in an equation of the form:

$$D = C_2(MW)^{-C_1}$$

where for dilute solutions of polyethylene glycol at 25°C, C_1 is 0.43 and C_2 is 5.16×10^{-5}.

independent of velocity will fundamentally change the perception of liquid chromatography as being an elegant but relatively slow separation technique to a tool which can be rapid while maintaining its separation capabilities. The surface chemistry which controls solute adsorption can now be considered independently from fluid transport phenomena, thereby simplifying the development of new chromatographic stationary phases.

Summary

The investigation of solute dispersion in LC has been the focus of many studies for both conventional spherical media as well as for continuous stationary phases, membrane chromatography systems and gigaporous particles. Since the first description of dispersion as a function of fluid velocity and physical parameters of packed beds by van Deemter, Zuiderweg, and Klinkenberg in 1956[2], many other researchers have sought to adapt and refine this type of model for dispersion phenomena which involve at least 5 major mechanisms of solute convection, diffusion, and sorption. Recent developments have given rise to stationary phases where intra- and extra- particulate convection is dominant over diffusional processes. The columns have the common characteristic of a plate height (i.e., peak dispersion) which levels off at high flow rates. Current research has defined plate height models which incorporate a velocity dependent term to describe effective diffusion in the intraparticulate void volume. The analysis of the literature presented in this paper suggests that flow processes involving forced convection within the intraparticle void volume can be described by a common plate height model which includes a velocity dependent, solute dispersion parameter.

Acknowledgments

The material in this work was supported by EM Separations Technology (Wakefield, RI, a U.S. Associate of E. Merck, Darmstadt, Germany) and NASA

(NSCORT) grant NAGW-2329. We thank Professors Phillip Wankat and Christine Ladisch, and Manish Gulati, and Joe Weil for helpful suggestions during preparation of this manuscript.

References

1. J. P. Martin and R. L. Synge, Biochem. J., 35, 1358 (1941).
2. J. J. van Deemter, F. J. Zuiderweg, and A. Klinkenberg, Chem. Eng. Sci., 5, 271 (1956).
3. J. C. Giddings, J. Chromatogr., 5, 47 (1961).
4. J. C. Giddings, J. Chromatogr., 5, 61 (1961).
5. E. D. Katz, K. L. Ogan and R. P. W. Scott, J. Chromatogr., 270, 51 (1983).
6. C. S. Horvath and H.-J. Lin, J. Chromatogr., 126, 401 (1976).
7. S. J. Hawkes, J. Chem. Ed., 60, 393 (1983).
8. J. C. Giddings, "Dynamic of Chromatography," Marcel Dekker, New York, 1965, Chapt. 2 and 3.
9. J. C. Giddings, "Unified Separation Science," Wiley, New York, 1991, Chapt. 12.
10. C. R. Wilke and P. Chang, AIChE J., 1(2), 264 (1955).
11. E. Grushka, L. R. Snyder, J. H. Knox, J. Chromatogr. Sci., 13, 25 (1975).
12. L. R. Snyder, J. Chromatogr. Sci., 7, 352 (1969).
13. L. R. Snyder, J. Chromatogr. Sci., 15, 441 (1977).
14. J. F. K. Huber and J. A. R. Hulsman, Anal. Chim. Acta, 38, 305 (1967).
15. J. F. K. Huber, J. Chromatogr. Sci., 7, 85 (1969).
16. G. J. Kennedy and G. H. Knox, J. Chromatogr. Sci., 10, 549 (1972).
17. J. N. Done, J. H. Knox, J. Chromatogr. Sci., 10, 606 (1972).
18. J. N. Done, G. J. Kennedy, J. H. Knox, in "Gas Chromatography 1972," S. G. Perry, ed., Appl. Sci. Publ., NY, 1973, p. 145.

19. C. S. Horvath and H.-J. Lin, J. Chromatogr., 149, 43 (1978).

20. W.-C. Lee, G.-J. Tsai, G. T. Tsao, Sep. Technol., 3, 178 (1993).

21. J. M. Miller, "Chromatography: Concepts and Contrasts," Wiley, New York, Chapt. 1, 2 and 9 (1988).

22. R. W. Stout, J. J. DeStefano, and L. R. Snyder, J. Chromatogr., 282, 263 (1983).

23. E. D. Katz, K. L. Ogan and R. P. W. Scott, in "The Science of Chromatography," J. Chromatogr. Library - Vol. 32, F. Bruner, ed., Elsevier, Amsterdam, 1985, p. 403.

24. H. Small, J. Colloid and Interface Sci., 48, 147 (1974).

25. G. Stegeman, J. C. Kraak and H. Poppe, J. Chromatogr., 634, 149 (1993).

26. R. N. Kelley and F. W. Billmeyer, Jr., Anal. Chem., 41, 874 (1969).

27. A. F. Hawkins, F. E. Regnier, and M. R. Ladisch, "Purification of Polyclonal IgG by pH Moderated Exclusion Chromatography," Paper 133, MBT Division, American Chemical Society, Los Angeles, CA, September 29, 1988.

28. A. F. Hawkins, "Purification of Human Polyclonal IgG by pH Moderated Size Exclusion Chromatography," MSE Thesis, Purdue University, May, 1990.

29. R. M. Chicz, Z. Shi, and F. E. Regnier, J. Chromatography, 359, 121 (1986).

30. N. B. Afeyan, N. F. Gordon, I. Mazsaroff, L. Varady, S. P. Fulton, Y. B. Yang, and F. E. Regnier, J. Chromatogr., 519, 1 (1990).

31. A. E. Rodrigues, J. C. Lopes, Z. P. Lu, J. M. Loureiro and M. M. Dias, J. Chromatogr., 590, 93 (1992).

32. D. D. Frey, E. Schweinheim and Cs. Horvath, Biotechnol. Prog., 9, 273 (1993).

33. M. E. van Kreveld and N. van den Hoed, J. Chromatogr., 149, 71 (1978).

34. Y. Yang, A. Velayudhan, C. M. Ladisch, and M. R. Ladisch, J. Chromatogr., 598, 169 (1992).

35. J. T. Thömmes, and M. -R. Kula, Biotechnol. Prog., 11, 357 (1995).

36. S. -Y. Suen, M. Caracotsios and M. R. Etzel, Chem. Eng. Sci., 48, 1801 (1993).

37. D. D. Frey, R. Van de Water and B. Zhang, J. Chromatogr., 603, 43 (1992).

38. S. -Y. Suen and M. R. Etzel, Chem. Eng. Sci., 47, 1355 (1992).

39. Y. Yang, A. Velayudhan, C. M. Ladisch and M. R. Ladisch, Adv. Biochem. Eng. Biotech., 49, 147 (1993).

40. G. Stegeman, R. Oostervink, J. C. Kraak, H. Poppe, and K. K. Unger, J. Chromatogr., 506, 547 (1990).

41. P. K. Cornel, R. S. Summers, P. V. Roberts, J. Colloid Interface Sci., 110, 149 (1986).

42. J. Brandrup, E. H. Immergut, ed., "Polymer Handbook," Wiley, New York, 1989, Chapt. VII.

43. J. F. Pfeiffer, J. C. Chen, and J. T. Hsu, *AIChE J.*, *42*(4), 932 (1996).

44. A. E. Rodriguez, L. Zuping, and J. M. Loureiro, *Chem. Eng. Sci.*, *46*(11), 2765 (1991).

45. Z. Lu, D. D. Frey, A. E. Rodriguez, *Ind. Eng. Chem. Res.*, *32*, 2159 (1993).

46. G. Carta, M. E. Gregory, D. J. Kirwan, and H. A. Massaldi, *Sep. Technol.*, *2*, 62 (1992).

47. V. Pretorius and T. W. Smuts, *Anal. Chemistry*, *30*(2), 274 (1966).

Appendix A. Supplemental Notation for Table II

A.1 Notation for the van Deemter Equation

γ = labyrinth factor, dimensionless (0.5 - 1.0)

λ = eddy diffusion factor, dimensionless

ε_m = fractional void volume of mobile (flowing) liquid phase

ε_s = fractional void volume of stagnant liquid phase

k = $K\frac{\varepsilon_m}{\varepsilon_s}$

K = distribution factor = $\frac{C_m}{C_s}$; also $C_m = KC_s$ represents a linear isotherm

NOTE: k and K are inverse of conventional definitions

C_m = concentration of solute in mobile liquid phase, units/m^3

C_s = concentration of solute in stagnant liquid phase, units/m^3

D_m = molecular diffusivity in mobile liquid phase, m^2/sec

D_s = molecular diffusivity in stagnant liquid phase, m^2/sec

A.2 Notation for the Giddings Equation

γ = obstruction factor, dimensionless (~0.6)

λ_i = convection factors

Φ = fraction of liquid phase within the support particle, dimensionless

R = equilibrium fraction of solute in mobile liquid phase

$$R = \frac{1}{1+k};\quad R = \frac{u_{sol}}{u_e}$$

k = capacity factor; ($k=K_D\Phi$)

K_D = distribution factor; $\left(K_D = \frac{C_s}{C_m}\right)$

γ' = obstruction factor for diffusion within the particle

A.3 Notation for the Huber and Hulsman Equation

τ_m = tortuosity of pores corresponding to ε_m

ε_m = fractional void volume in which flow occurs

λ_1,λ_2 = constants characterizing the bed geometry

k = $\frac{\varepsilon_s}{\varepsilon_m}K$

$K = \frac{C_s}{C_m}$

τ_s = tortuosity of pores corresponding to ε_s

ε_s = fractional void volume of stagnant liquid

D_m = diffusivity of solute in mobile phase

D_s = diffusivity of solute in stagnant liquid phase

ν_s = kinematic viscosity of mobile phase

A.4 Notation for Knox Equation

See "Notation for Giddings Equation"

A.5 Notation for Horvath and Lin Equation

$\gamma,\lambda,\omega,\kappa$= structural parameters of the column packing

k' = mass distribution ratio (capacity factor) = ϕK

K = $C_s / \Lambda C_m$ (for linear chromatography)

$k_o = \frac{\varepsilon_s}{\varepsilon_m}$

Λ = concentration of active sites accessible to eluite molecules

θ = tortuosity factor

ϕ = phase ratio

A.6 Notation for the Extended van Deemter Equation

This notation comes from Grushka, Knox, and Snyder (1975).

γ,λ,ω,q= structural parameters related to bed geometry

$f(k)$ = some function of the capacity factor

k = capacity factor = $K\frac{V_s}{V_m}$

K = partition coefficient = $\frac{C_s}{C_m}$

V_s = volume of stationary phase

V_m = volume of mobile phase

D_m = diffusion coefficient of solute in mobile phase

D_s = diffusion coefficient of solute in stationary phase

d_p = particle diameter

d_f = film depth of stationary phase

Appendix B. Supplemental Notation for Table III

a = radius

b = capacity factor

Bi_m = Biot number ($= k\ \ell/D_{eff}$)

D_{eff} = intraparticle effective diffusivity ($= \varepsilon_p D_p$)

D_{ax} = axial dispersion coefficient

D_p = pore diffusivity

K_f = film mass transfer coefficient

ℓ = half thickness of slab

L = bed length

$\tilde{L}_d$ = time constant for intraparticle diffusion ($= \ell^2/D_p$)

$\tilde{L}$ = space time ($= L/u_o$)

$$M = \frac{\varepsilon_p(1-\varepsilon)b^2L}{3\left(\varepsilon + b\varepsilon_p(1-\varepsilon)\right]^2}$$

P_e = Peclet number ($= v_o L/\varepsilon D_{ax}$)

u_o = superficial velocity

v_o = intraparticle convective velocity

ε = bed porosity

ε_p = particle porosity

α = dimensionless bed porosity = $\tilde{L}_d / \tilde{C}$

$$\bar{v} = \frac{2av}{D} \text{ (reduced velocity)}$$

λ = intraparticle Peclet Number = $\frac{v_o \ell}{D_{eff}}$

λ_R = $\frac{v_o a}{D_{eff}^3}$ (where a = particle radius)